ELSEVIER

Polymer 43 (2002) 185–193

polymer

www.elsevier.com/locate/polymer

Linking the atomistic scale and the mesoscale: molecular orbital and solid state packing calculations on poly(*p*-phenylene)☆

Ioannis Rabias[a,1], Cyril Langlois[b,2], Astero Provata[b], Brendan J. Howlin[a,*], Doros N. Theodorou[b,c]

[a]*Department of Chemistry, School of Physics and Chemistry, University of Surrey, Surrey, Guildford GU2 5XH, UK*
[b]*Institute of Physical Chemistry, NRCPS Demokritos, 15310 Athens, Greece*
[c]*Department of Chemical Engineering, University of Patras, 26500 Patras, Greece*

Abstract

The energies and structures of neutral benzenoid and neutral quinonoid polyphenylenes in the gas phase were calculated at the ab initio and semi-empirical levels for oligomers containing up to 11 rings as a function of the torsion angles between consecutive aromatic rings. In the gas-phase poly(*p*-phenylene) (PPP) simulations, a transition to the aromatic benzenoid structure occurs in the centre of chains as short as about six to seven rings. The development of electronic properties such as ionisation potential, the carbon–carbon bond length between rings, the band gap and width of the highest occupied bands were studied. On going from a coplanar to a perpendicular conformation, qualitatively, the ionisation potential and band gap values increase and the band widths of the highest occupied bands decrease. Molecular mechanics simulations were used to model the crystal structures of PPP oligomers using Lennard–Jones and sinusoidal torsion potentials, with parameters derived initially from the gas-phase calculations. These solid state simulations reproduced known crystal structures and predictions are made for the crystal structures of PPP oligomers up to a degree of polymerisation of 11. The crystal packing forces the PPP molecules to be planar, hence increasing conductivity in the solid state. Interestingly, there is an anomaly in the packing energy results for the sexiphenylene case which is in accord with the gas phase calculations. © 2001 Elsevier Science Ltd. All rights reserved.

Keywords: Molecular orbital; Ab initio; Molecular mechanics

1. Introduction

From the large class of poly-conjugated aromatic polymers, which upon doping with electron donors or electron acceptors display metallic conductivities, poly(*p*-phenylene) (PPP) is one of the experimentally most investigated systems. Nevertheless, detailed information on the microstructure of the doped materials is at present not available from the experimental side because of substantial structural and chemical disorder, inhomogeneities in the degree of polymerisation, and the simple fact that the structure varies with the amount of doping [1].

As with the other members of this currently very actively investigated family of compounds, e.g. polypyrrole and polythiophene, charged, doping-induced defects, either in the form of anion or cation radicals (polarons) or of dianions or dications (bipolarons), were suggested as being the relevant charge carriers in the electric transport processes of the doped materials. Because of the inherent difficulties in obtaining good-quality polymer samples, new synthetic routes [2,3] and the systematic experimental investigation of oligomer properties are still being intensely pursued [1,4].

One of the main questions addressed in this work is how the equilibrium structures of the neutral benzenoid and the neutral quinonoid isolated oligomers converge upon increasing the chain length. A characteristic usually associated with π-conjugation is the planarity of the compound, which favours a maximum overlap between the π atomic orbitals. It was, however, quickly realised that some of the unsaturated organic polymers, which can be made conducting on doping, possess chains that are not in a coplanar

☆ This paper was originally submitted to *Computational and Theoretical Polymer Science* and received on 22 January 2001; received in revised form on 16 July 2001; accepted on 19 July 2001. Following the incorporation of *Computational and Theoretical Polymer Science* into *Polymer*, this paper was consequently accepted for publication in *Polymer*.

* Corresponding author. Tel.: +44-1483-876-834; fax: +44-1483-876-851.

E-mail addresses: aprovata@limnos.chem.demokritos.gr (A. Provata), b.howlin@surrey.ac.uk (B.J. Howlin).

[1] Present address: Department of Chemical Engineering, University of Thessaloniki, 54006 Thessaloniki, Greece.

[2] Present address: Department of Chemical Engineering, University of Patras, 26500 Patras, Greece.

0032-3861/02/$ - see front matter © 2001 Elsevier Science Ltd. All rights reserved.
PII: S0032-3861(01)00587-0

conformation. This is especially true in the case of polymers based on rings such as PPP($-C_6H_4-)_n$, for $n = 5$. In PPP, steric interactions between hydrogen atoms in *ortho* positions result in the appearance of a small torsion angle between two adjacent phenyl rings approximately equal to $\pm 22.7°$ with every other ring lying in the same plane [5–7].

The ionisation potential (IP), band gap (Eg), and bandwidth (BW) values are very important in the context of the conducting polymer area. The band gap value determines the intrinsic electrical properties of the material, and when subtracted from the ionisation potential, it provides the electron affinity, which is important with regard to the *n*-type doping process. The ionisation potential value indicates whether a given dopant is capable of ionising the polymer chains. The bandwidth of the highest occupied band gives an idea of the electronic delocalisation along the chains and can be roughly correlated with the mobility of possible charge carriers appearing in that band.

These parameters are really only obtainable from an extended solid state molecular orbital calculation on PPP but in the literature some progress has been made by performing molecular orbital calculations on isolated dimers or oligomers and extrapolating the parameters calculated from these systems to the infinite size limit which corresponds to experimental situations. There is undoubtedly a degree of error in this approach, which depends on how sophisticated the approach taken is. We thus have confined ourselves to comparisons of observed trends instead of absolute values. There has been extensive investigation of the energetics and structures of poly(*p*-phenylenes). Recently, Jing-Fang Pan, Soo-jin Chua and Wei Huang reported a study on the variation of torsional angles in side chain substituted biphenyls [8]. They used the semi-empirical MOPAC program with the AM1 and PM3 Hamiltonians and ab initio molecular orbital calculations with an MP2/6-31G** basis for comparison. There was a difference in the results produced by these methods. The ab initio and AM1 calculations gave inter-ring torsion angles of 51 and 40°, respectively, in the gas phase, whereas PM3 gave 0°. They concluded that this was due to an underestimation of the steric repulsion between the *ortho*-hydrogen atoms in the PM3 Hamiltonian. These results are in good agreement with theoretical studies of biphenyl [9] and PPP [10] and experimental results on PPP oligomers [9] and isolated polymer chains [11].

This work reports a combined theoretical investigation into both the gas phase structure of oligomers of PPP and their solid state packing. The gas-phase calculations are used to inform the solid-state experiments. The influence of the torsion angle along the chains has been well documented as having an effect on the electronic and geometric structures of oligomers of PPP in the gas phase (see preceding paragraph). By varying the torsion angle between adjacent rings from a coplanar conformation to a perpendicular conformation it is possible to study, qualitatively at least, the development of the length of the carbon–carbon bond between rings, the ionisation potential, the band gap and the width of the highest occupied electronic bands. A major aim of this study was to explore the influence of the torsion angle on the solid-state packing. Would the packing energy overcome the torsion potential, or vice versa? Experimental studies indicate that the torsion angles in the solid state are reduced by at least 20° from the gas phase structures [12–14].

The solid state calculation on PPP oligomers was undertaken using molecular mechanics simulation. The solid phase modelling of $(PPP)_n$ with n ranging from four to seven is presented. The cases where $n = 10$ and 11 are also considered, in order to predict experimental diffraction results, which are not available this far. As in the gas phase calculations, the torsion angles were taken into account as degrees of freedom. The molecular mechanics technique, using software written in house, was chosen to minimize the energy of the structure. Lennard–Jones and sinusoidal torsional potentials [15] were used in these calculations, with parameters derived initially from the gas phase calculations. The energy of a periodic cell containing several molecules was obtained. By minimizing the energy, the equilibrium structure of the crystal was found. Our solid state simulations are shown to reproduce the known crystal structures and predict the structural properties of crystalline larger oligomers ($n = 10, 11$).

Section 4 presents a cumulative discussion of the gas phase and solid state results and a comparison with available experimental data.

2. Computational methods

Molecular orbital calculations were performed on MOPAC V6.0 and GAUSSIAN 94 using the QM Utilities interface in Molecular Simulations' CERIUS^2 package [16]. Initial models of PPP oligomers were constructed using the 3D-Builder module in CERIUS^2. Gaussian calculations using a 3-21G basis set were performed on neutral benzenoid $(PP)_n$ and quinonoid $(QPP)_n$ oligophenyls for $n = 2$–11, in the gas phase. A schematic structure of the oligomer for the case $n = 3$ is shown in Fig. 1. The torsion angle between the rings was varied from 0–90° in separate calculations on the oligomers. Calculations are presented for 0, 20, 40, 60 and 90°. Calculations on the evolution of the carbon–carbon bond length between rings as a function of the torsion angle were performed at the ab initio Hartree–Fock 3-21G and semi-empirical AM1 and PM3 levels on the oligomers. All subsequent analyses of the calculations were also performed with the QM Utilities Interface to visualise eigenvalues and eigenvectors. Calculations were carried out on a Silicon Graphics INDY R6000 running IRIX 5.2. A single basis set was chosen for the Gaussian calculations to provide the best compromise between accuracy and speed.

The atomistic calculations were used to provide parameters

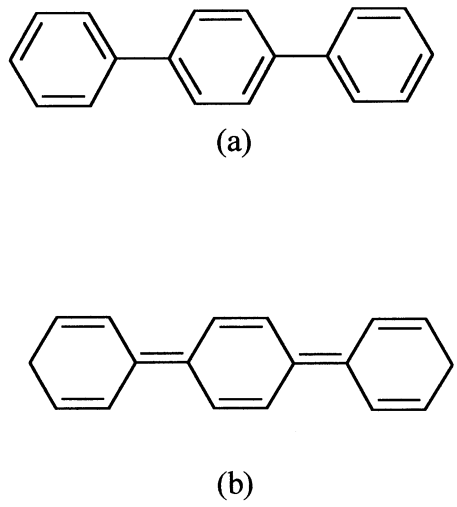

Fig. 1. Structures of (a) planar terphenyl, 3PP, and (b) its quinonoid counterpart, Q3PP.

for the solid-state calculations. For the solid state calculations, crystal cells containing six molecules with periodic boundary conditions were equilibrated using Molecular Mechanics (software written in house). The molecules considered contained a number of phenyl groups ranging from $n = 2$ to $n = 11$. In the calculations, a classic Lennard–Jones [15] potential was chosen for the representation of the intermolecular interactions and a sinusoidal torsional potential for the interactions between adjacent phenyl rings. To obtain the equilibrium structures, the energy of the cell was minimised up to a given energy gradient ut-off. Detailed presentation of the potentials and calculations are presented in Section 3.2 The solid state packing calculations were run on a INDY R5000 running IRIX 5.2 (solid state software available upon request).

3. Results and discussion

3.1. Gas phase calculations

Because of the large size of the systems treated, the double-type 3-21G basis set was used throughout as it had been successfully applied in the calculations of Cuff and Kertesz [17] on neutral terphenyls of PPP. Currently and taking into account the limitations in available computing facilities, the size of the systems precludes the study of solvents or the use of significantly more extended basis sets or of sophisticated methods. However, most of the errors encountered as a consequence of the application of this comparatively small basis set may be assessed easily by comparing the computed structural and energetic data for biphenyl with experimental structures [3] and with results of more advanced calculations from other authors [5–7]. Moreover, it is to be expected that these errors are highly systematic and therefore common to all models treated.

The benzenoid and quinonoid models were treated as conventional closed-shell systems. In general, all computed equilibrium structures were under the constraint of planarity, i.e. D_{2h} symmetry. Non-planar equilibrium structures, with the restriction to D_2 symmetry, were also considered up to $n = 5$.

No calculations on the charged systems have been done; the counterions were not taken into account for the following reasons: (i) the explicit interaction between the dopants and the polymer chain are not correctly described at the self-consistent field level, (ii) the complete symmetry optimisation of the longer oligomers, including counterions, is exceedingly complicated because there are several minima for each oligomer.

The number and the size of the molecules treated atomistically are sufficiently large to preclude the reporting of all the various computed equilibrium structures in full detail. Instead, the discussion is restricted to the most important trends in the regularisation of the optimised C–C bond lengths occurring upon chain length elongation. In this work, not only the length of the bond between the rings was optimised but also all bond lengths and bond angles within the rings, see Table 1 and Fig. 2 for selected results. The geometrical parameters were initially set at the values computed from 3-21G geometry optimisations on the dimer. The optimised geometries found from the calculations inside the rings are in very good agreement with the available X-ray, neutron, or electron diffraction data on the poly(*p*-phenyl) oligomers [5–7]. These calculations have been used to provide qualitative values for comparing the ionisation potential (IP), band gap (Eg), and bandwidth (BW) in the oligomers studied. The ionisation potential was estimated by taking the negative of the HOMO orbital energy. It should be noted that the application of Koopmans theorem in this way provides an accuracy of approximately 1 eV. The band gap is approximated by taking the difference between the energies of the highest occupied molecular orbital (HOMO) and the lowest unoccupied molecular orbital (LUMO) and its value is strongly dependent on the basis set chosen.

The structural parameters of a phenyl ring converge upon increasing the chain length in the neutral benzenoid oligophenyl series. With the exception of the terminal rings, the

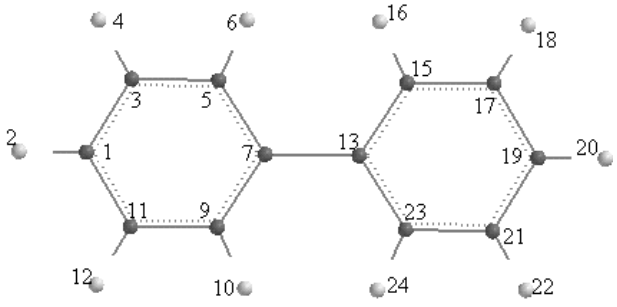

Fig. 2. Representation of the numbering of atoms of biphenyl.

Table 1
Geometry of the atoms in biphenyl derived from MOPAC using PM3

Atom	Bond length, X(Å)	Bond angle, Y (°)	Torsional angle, Z (°)	Atom	Atom	Atom
C7						
C13	1.471			C7		
C15	1.403	119.98		C13	C7	
C17	1.394	120.54	−179.9	C15	C13	C7
C19	1.395	119.73	0.2	C17	C15	C13
C21	1.395	120.18	0.0	C19	C17	C15
C23	1.402	120.88	−179.5	C13	C7	C15
H24	1.101	119.64	−179.7	C23	C13	C21
H22	1.100	120.04	179.8	C21	C19	C23
H20	1.100	119.3	179.9	C19	C17	C21
H18	1.099	120.09	−179.9	C17	C15	C19
H16	1.101	119.64	−179.4	C15	C13	C17
C5	1.402	120.58	40.1	C7	C13	C15
C3	1.393	120.75	179.5	C5	C7	C13
C1	1.395	120.02	0.0	C3	C5	C7
C11	1.395	119.64	0.1	C1	C3	C5
C9	1.402	120.65	179.5	C7	C13	C5
H10	1.100	119.85	−179.5	C9	C7	C5
H12	1.100	119.87	179.4	C11	C1	C9
H2	1.099	120.21	180.0	C1	C3	C11
H4	1.100	119.90	−179.8	C3	C5	C1
H6	1.101	119.55	−179.7	C5	C7	C3

intra- and inter-ring C–C distances of the central phenyl ring dimer differ by no more than 0.001 Å. This difference can be considered insignificant with the basis set used. Bearing this in mind most of the comments in this work will be concerned with comparison of the behaviour of the oligomers over the entire series studied. Of particular interest is the structural behaviour in the QnPP series. The quininoid bond length alternation pattern is stable up to $n = 5$ only; for larger n, the benzenoid bond length alternation pattern appears abruptly, showing essentially already all the structural features encountered for Q10PP. Only the outermost ring displays a quinonoid structure, whereas all the interior rings are benzenoid. It must be borne in mind that, strictly, all the QnPP systems with $n > 5$ should more correctly be described as bi-radicals. The computed total energies (per phenyl ring) of all the D_{2h}-optimised oligophenyl species treated in this work, are collected in Table 2. These energies may conveniently be used in a spreadsheet manner to illustrate the various regularities in the convergence behaviour of these series. For each one of the series one may define:

$$\Delta E(n\text{PP}) = E(n\text{PP}) - E[(n-1)\text{PP}]$$

$$\Delta E(\text{Q}n\text{PP}) = E(\text{Q}n\text{PP}) - E[\text{Q}(n-1)\text{PP}]$$

Eliminating the energy per phenyl unit:

$$\Delta\,\Delta E(\text{Q}n\text{PP}) = \Delta E(\text{Q}n\text{PP}) - \Delta E(n\text{PP})$$

Obviously, for large n, $\Delta\,\Delta E$(QnPP) converges to zero so it is more interesting to look at the behaviour of the $\Delta\,\Delta$(QnPP) over the complete series of oligomers studied. As has already been discussed, in the computed equilibrium structures of the QnPP species (see Fig. 1), the quinonoid bond-length alternation pattern is unstable for $n > 5$. For larger n, the benzenoid structure prevails in the centre of the oligomers. This behaviour is also apparent in the corresponding total energies and also in the energy differences. Between $n = 6$ and $n = 7$, $\Delta\,\Delta E$(QnPP) shows a sharp transition. As long as the quinonoid structure remains stable, $\Delta\,\Delta E$(QnPP) represents the energy difference between the benzenoid and the quinonoid ring, which was found to be around 88 kJ mol^{-1} for $n = 3$. For larger n, $\Delta\,\Delta E$(QnPP) quickly approaches zero.

Table 2
Total energies of optimised benzenoid (nPP), and quinonoid (QnPP) oligophenyls and $\Delta\,\Delta E$(QnPP) divided by the number of phenyl rings as obtained at the 3-21G SCF level

n (number of phenyl rings)	Optimised energy E(nPP) (hartree)	Optimised energy E(QnPP) (hartree)	$\Delta\,\Delta E$(QnPP) (hartree)
1	−229.40	−305.80	−76.40
2	−228.80	−267.00	−38.20
3	−228.60	−254.10	−25.50
4	−228.50	−247.62	−19.12
5	−228.48	−243.74	−15.26
6	−228.45	−241.15	−12.70
7	−228.42	−239.31	−10.89
8	−228.40	−237.94	−9.54
9	−228.38	−236.85	−8.47
10	−228.38	−236.00	−7.62
11	−228.36	−235.27	−6.91

Table 3
Evolution, as function of the torsion angle between the rings, of the 3-21G, PM3 inter-ring bond length, in Å, for biphenylene (*n*PP) $n = 2$

Angle (°)	*n*PP(3-21G)	*n*PP(PM3)
0	1.469	1.471
20	1.466	1.465
40	1.460	1.460
90	1.466	1.465

These $\Delta\,\Delta E(n)$ values had previously [17] been used in the work of Cuff and Kertesz to determine, exclusively with the aid of molecular calculations, which of the two structure types, benzenoid or quinonoid, will be the preferred one in a given polyconjugated polymer. They concluded that should the energy difference be too small, then one simply has to expect disorder. Therefore, one cannot use this relationship to determine the critical oligomer length at which the structural transition occurs in the centre.

The crystal packing calculations, presented in Section 3.2, justify the use of the planar D_{2h} structures, as the following short discussion of a few results obtained on D_2 and D_{2h} structures illustrates: the neutral, D_{2h}-optimised *n*PP species $n = 2$ to $n = 5$ share an approximate energy difference to the more stable, planar D_2 structures of about 15 kJ mol^{-1} per inter-ring bond. In the latter, optimised inter-ring torsion angles of 50° were obtained. In a recent, methodologically superior calculation [18] at the 6-3lG* basis set on biphenyl, a very similar energy difference of around 14.5 kJ mol^{-1} between the D_2 and the D_{2h} conformation, together with an optimal torsion angle around 46° were found. All the D_{2h}-optimized Q*n*PP species for $n = 2$–5 are minima. However, despite this energy difference in the gas phase for the shorter oligomers, in the calculations of the larger oligomers, especially in the solid state, the planar conformations were used since the crystal packing finally forces the decrease of the torsion angles towards zero.

In biphenyl, the most stable conformation arises when the torsion angle is between 0 and 40°; in this study the results are 40° for AM1 and 0° for PM3. It should be noted that PM3 has been shown to give wrong results for biphenyl [19]. The gaseous biphenyl [20] gives an estimate from diffraction data of 42° for this torsion angle whilst ab initio double-ζ calculations [19] predict 32° and molecular mechanics calculations yield 39° [21]. Both the 40° torsion and the perpendicular conformations are about 0.5 kJ mol^{-1} less stable than the coplanar angle situation at the 3-21G level and about 8.4 kJ mol^{-1} less stable at the molecular mechanics level [21]. The double-ζ calculations result in the 40° torsion and perpendicular conformations being, respectively, 7.56 and 18.9 kJ mol^{-1} less stable than the optimal conformation [19]. In the solid state, crystal packing effects result in a decrease of the torsion angle to 22.7°. The main reason behind the larger stability of a twisted conformation has to be found in the steric interactions between the hydrogen atoms in *ortho* positions. For a 0° torsion angle, the shortest distance between two *ortho* hydrogens belonging to different rings is only of the order of 1.9 Å, which goes up to about 2.4 Å when the twist angle increases to 40°.

The dependence of the bond length between the rings on the torsion angle is presented in Table 3. In all molecules, the most stable conformation leads to the shortest inter-ring bond length. In the case of biphenyl, the shortest bond length found for 0° is 1.471 Å and for the 40° torsion angle conformation the shortest bond length is equal to 1.460 Å. As the rings go toward a more coplanar conformation, the inter-ring bond length elongates in order to compensate, at least partly, for the increasing steric interactions between *ortho* hydrogens and eventually reaches 1.471 Å. Identical trends are found at the double zeta basis set level [22]. It is interesting to examine the 3-21G bond orders, as obtained from a Mulliken population analysis, in the coplanar conformation. Within the rings, the π contributions to the total carbon–carbon bond orders range between 22 and 28%. For the inter-ring bond order, the π contributions are only of the order of 5%. This is consistent with the fact that the inter-ring bond in biphenyl is essentially a single bond between sp^2 carbons, whose standard length is usually considered to be about 1.50–1.51 Å. Experimentally, the inter-ring bond [5–7] is estimated to be 1.50 Å. The IP is simply approximated by taking the negative of the energy of the HOMO. As the torsion angle increases, so does the calculated ionisation potential value, as expected. The perpendicular conformation yields a value of the ionisation potential that is 1.3 eV larger than that for the coplanar situation. The evolution of the ionisation potential up to a torsion angle of 90° can be very well fitted by a cosine function, as illustrated in the following equation:

$$\mathrm{IP}_\chi = \mathrm{IP}_0 + [(\mathrm{IP}_{90} - \mathrm{IP}_0)(1 - \cos\chi)],$$

where IPχ is the ionisation potential value for a torsion angle of χ°. This indicates that the electronic interaction between the rings, as far as the highest occupied levels are concerned, decreases in the same way as the overlap between the π atomic orbitals on adjacent rings. For the 40° torsion angle conformation, the IP has increased only by some 0.35 eV with respect to the 0° case.

In these conjugated molecules, the HOMO in the coplanar conformation of course has π character (see Fig. 3). In biphenyl, our results indicate a 0.36 eV increase in the IP value when going from the coplanar case to the 40° torsion angle situation. In Table 4, the evolution of the bond length and ionisation potential as a function of torsion angle along the chains is presented. The band gap, and the bandwidth of the highest occupied bands for the *p*-phenylene pentamer, is 1.5–2.0 eV. By comparing the results for the 0 and 20° torsion angles in Table 4, one concludes that a 22.7° twist has only a small effect on the electronic properties that are believed to be of importance in conducting polymers. This is also indicated in the AM1 results, where, with respect to the coplanar conformation, the IP is

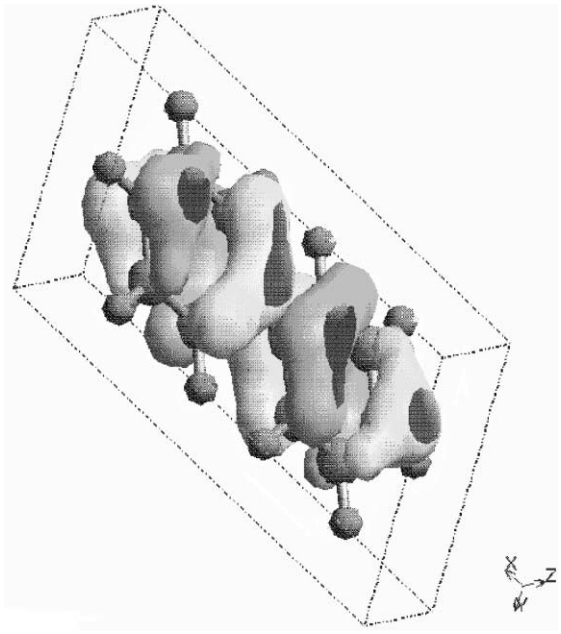

Fig. 3. Representation of the highest occupied molecular orbitals (HOMOs) of biphenyl.

higher by 0.1 eV and the band gap by 0.2 eV. The calculated 7.2 eV IP at 0° in this work for PPP agrees well with the 7.0–7.1 eV experimental estimate [3]. The differences between the ionisation potentials at 0 and 90° torsion angles is, as could be expected, due to greater overlapping of orbitals at 0°. However, the energy gap and the bandwidth increase over this range of torsion angles for exactly the same reason.

3.2. Solid state calculations

In the solid state simulations, only torsion angles were taken as degrees of freedom. Thus, all the other parameters were fixed with respect to the experimental data and former investigations of PPP [23]. The phenyl rings are represented as perfect hexagons, which seems to be a reasonable approximation as is shown in Table 1. Also, the inter-ring bond length has been fixed, with regard to the data of Table 1 and the experimental diffraction data [23]. The three different bond lengths that come into play here are summarized in Table 5. The positions of the molecules in the crystalline cell were based on the crystallographic data available for those molecules [23]. The crystal structure of biphenyl belongs to the monoclinic system and the space group $P2_1/a$-(C_{2h}) with two molecules per cell, $a = 7.82$ Å, $b = 5.58$ Å, $c = 9.44$ Å, and $\alpha = 94.620°$. With respect to these data, the positions of the molecules are fixed and only the rotations of the rings around their molecular axes are allowed. A periodic crystal structure (periodic cell) containing $1 \times 3 \times 2$ crystalline cells has been considered, which contains six molecules (Fig. 4). The periodic cell size was chosen to ensure the simulation of an almost cubic box. The crystallographic data used in this part are given in Table 6 for a monoclinic unit cell, with cell lengths a, b, c and cell angles α, β, γ. The potentials used in this molecular simulation are [15,24] a torsional potential, depending only on dihedral angles governing the inter-ring bonds, and an intermolecular potential.

Table 5
Values of the bond lengths in Å from the modelling

Molecule	C–C intracycle	C–H	C–C intercycle
p-Quaterphenylene	1.37	0.95	1.48
p-Quinquephenylene	1.37	0.95	1.48
p-Sexiphenylene	1.37	0.95	1.48
p-Septiphenylene	1.38	0.95	1.49
p-Decaphenylene	1.38	0.95	1.49
p-Endecaphenylene	1.38	0.95	1.49

(i) The torsional potential U has a sinusoidal shape, which tends to make the molecule planar, in order to represent the packing forces of the crystal:

$$U(\varphi(j)) = V/2[1 - \cos(2\varphi(j))]$$

The value of V used was 25 kcal mol^{-1} (104.5 kJ mol^{-1}). It should be noted that the torsional force constant derived from the ab initio calculations presented earlier is much less than this figure, but it is important in the use of force-field calculations like this to balance the parameters. The objective of this force constant was to correctly reproduce known crystal structure data.

Table 4
Evolution, as a function of the torsion angle between adjacent rings at the PM3 and AM1 levels of the ionisation potential (IP), band width (BW) and band gap (Eg), of highest occupied bands in biphenyl

Angle (°)	IP(AM1) (eV)	IP(PM3) (eV)	BW(AM1) (eV)	BW(PM3) (eV)	Eg(AM1) (eV)	Eg(PM3) (eV)
0	7.20	7.20	3.80	3.79	3.44	3.44
20	7.30	7.30	3.50	3.47	3.44	3.60
40	7.55	7.56	2.71	2.73	4.20	4.20
60	7.99	8.00	1.70	1.69	5.10	5.10
90	8.50	8.51	0.20	0.18	5.63	5.65

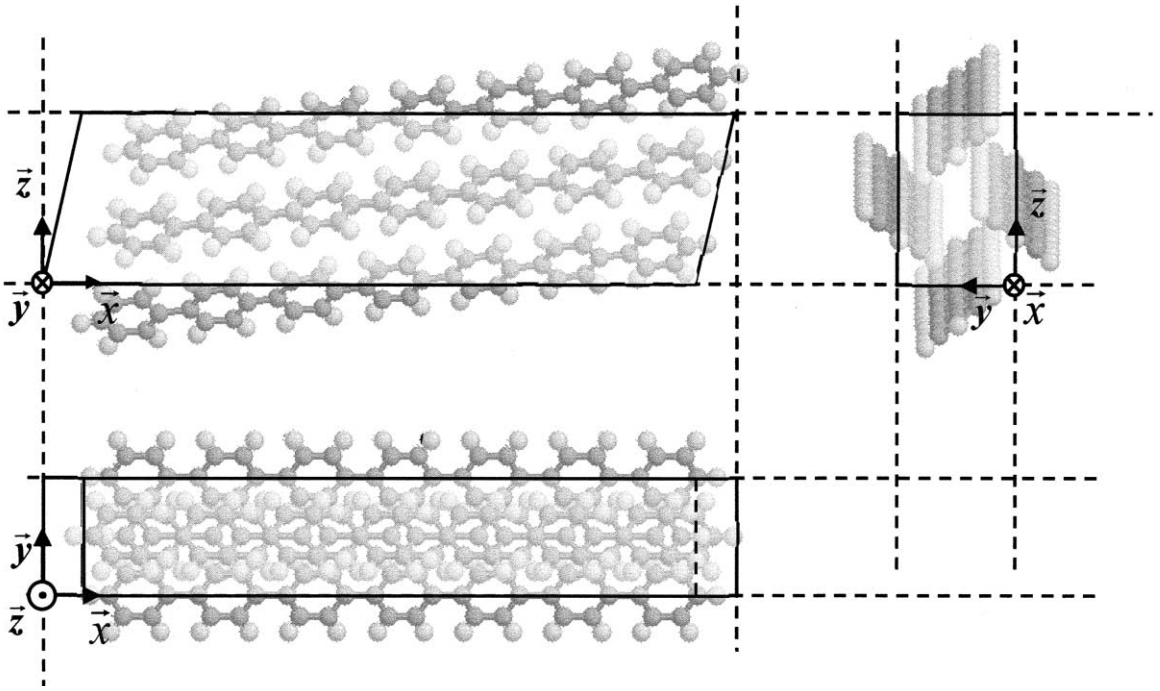

Fig. 4. Representation of the monoclinic crystalline cell of planar septiphenyl.

(ii) The intermolecular potential is a classical Lennard–Jones potential [15,24] with a set of constants σ and ϵ depending on the type of the interaction and on the distance r between the atoms considered. The values chosen for σ and ϵ are shown in Table 7.

With these potentials, the energy of the system can be minimized with respect to the degrees of freedom to find the equilibrium stucture. The Broyden–Fletcher–Goldfarb–Shanno (BFGS) Quasi–Newton method [25], using only first derivatives of the degrees of freedom, has been used for all the poly(*p*-phenylenes) studied. This method has converged for half of the structures studied to local minima and has oscillated around the minima for the other half. The main convergence criterion is to obtain the gradient of energy with respect to the degrees of freedom lower than 10^{-4} kcal degree^{-1}. Nevertheless, the accuracy was enough in all the cases to get the equilibrium structure of the system.

The main observation of the molecular mechanics calculations of the solid phase is that the molecules of PPP are planar (Fig. 4). The greatest deviation of a dihedral angle from planarity does not exceed 0.5° and the mean of the angles is 0°, with a precision of 10^{-4}. This tendency occurs for all the values of n and is in perfect agreement with the diffraction data [23]. As an example, see the results in Table 8 for quinquephenyl. The planarity of the molecules in the solid state is of great importance for electronic conduction.

The second observation is the orientation of the molecules in the crystalline cell. For a molecule, we define an orientation angle ψ_3 by considering the angle between the plane of the first angle of the chain and the plane defined by: (i) the axis of the molecule, and (ii) the projection of this axis on the (O, X, Y) plane (Fig. 5).

For each cell, two different orientation angles ψ_{31} and ψ_{32} are shown because the two molecules do not have the same orientation in the cell. Therefore, in the periodic cubic cell of six molecules under consideration, we can average the two different orientation angles (Table 9). The values in Table 9 include the experimental ones for ease of comparison. It is obvious that for the ψ_{31} angles, the values are in good agreement. An increase in ψ_{31} with the degree

Table 6
Monoclinic unit cell parameters; values for the two last rows are from extrapolations

Molecule	a (Å)	b (Å)	c (Å)	α (°)	β (°)	γ (°)
p-Quaterphenylene	17.91	5.610	8.110	90	95.8	90
p-Quinquephenylene	22.056	5.581	8.070	90	97.91	90
p-Sexiphenylene	26.241	5.568	8.091	90	98.17	90
p-Septiphenylene	30.577	5.547	8.034	90	100.52	90
p-Decaphenylene	43.211	5.497	8.001	90	106.43	90
p-Endecaphenylene	47.435	5.479	7.984	90	108.32	90

Table 7
Constants used in the Lennard–Jones potentials for the three different types of interaction

Constants	σ (Å)	ϵ (kcal mol^{-1})
C–C	3.006788	0.039521
C–H	2.56132	0.035309
H–H	3.35	0.032382

Table 8
Example of the solid state packing cell constants obtained for quinquephenylene

Angle (°)	Cell 111	Cell 112	Cell 121	Cell 122	Cell 131	Cell 132
ψ_{31}	**54.19**	**54.18**	**54.19**	**54.18**	**54.19**	**54.18**
ϕ_{12}	0.13	0.13	0.13	0.13	0.13	0.13
ϕ_{13}	0.02	0.02	0.02	0.02	0.02	0.02
ϕ_{14}	−0.02	−0.02	−0.02	−0.02	−0.02	−0.02
ϕ_{15}	−0.13	−0.13	−0.13	−0.13	−0.13	−0.13
ψ_{32}	**125.82**	**125.81**	**125.82**	**125.81**	**125.82**	**125.81**
ϕ_{22}	−0.15	−0.13	−0.15	−0.13	−0.15	−0.13
ϕ_{23}	−0.02	−0.02	−0.02	−0.02	−0.02	−0.02
ϕ_{24}	0.02	0.02	0.02	0.02	0.02	0.02
ϕ_{25}	0.15	0.13	0.15	0.13	0.15	0.13

Table 9
Mean values of ψ_{31} and ψ_{32} in the periodic cubic cell and ψ_{31} and ψ_{32} from diffraction data

Molecule	ψ_{31} (°)	ψ_{32} (°)	ψ_{31} (diffraction) (°)	ψ_{32} (diffraction) (°)
p-Quaterphenylene	54.11	125.86	56.5	101.5
p-Quinquephenylene	54.19	125.81	56.5	99.5
p-Sexiphenylene	54.27	125.79	55	116
p-Septiphenylene	54.99	125.02	57	96.5
p-Decaphenylene	56.03	123.96	(not vailable)	(not available)
p-Endecaphenylene	55.83	124.10	(not available)	(not available)

of polymerization, n, is also observed, if we exclude sexiphenylene, which has special properties [23], as seen in the gas phase calculations and experiment. These results indicate that if one wants to take this transition into account in molecular mechanics calculations, one needs to modify the potentials, as this electronic effect is not easily modelled using standard Coulombic point charge potentials. As for ψ_{32}, the simulation values diverge from the experimental by almost 30°, although the tendency of decreasing with increasing n is respected. Again, sexiphenylene is an exception to this tendency. The ψ_{31} angle increases, as it does in the experiment with the exception of sexiphenylene where there is an abrupt anomaly. This exception can be understood in terms of the gas phase results which indicate a transition between quinonoid and benzenoid natures at the sexiphenylene stage. Furthermore, Table 9 indicates that ψ_{31} and ψ_{32} add up to 180°, which is expected owing to the symmetry of the Lennard–Jones interactions. This is not the case in the experimental results (see Table 9, diffraction data), as there is an effect of disorder (the mosaic nature of real crystals).

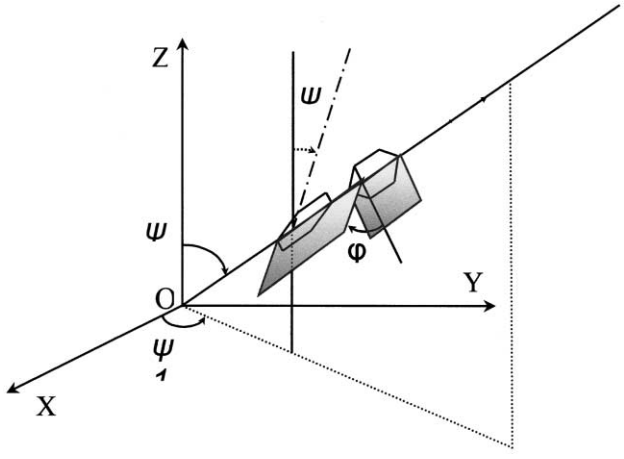

Fig. 5. Definition of the different angles needed for the simulation.

4. Conclusions

Complementary studies of gaseous and solid-state PPP have been undertaken using microscopic 3-21G, AM1, PM3 molecular orbital methods and mesoscopic molecular mechanical methods. Systematic calculations of the structures and of the energetics in oligophenyls of sizes $n =$ 2–11, where n is the number of phenyl rings, were performed.

By considering the series of neutral oligophenyls, *n*PPP, and model molecules Q*n*PPP, a distinct energy difference between the oligophenyls was observed in the gas phase calculations. The reason for this behaviour lies in the substantially larger energy difference between benzenoid and quinonoid valence isomers in the case of the gas phase PPP series. Because of this larger energy difference, it is energetically more unfavourable to sustain the quinonoid structure over a larger spatial region. The trends in the ionisation potential, band, width and energy gap were studied as a function of the torsion angle along the chains and demonstrated the evolution of electronic properties,

which are of interest in conducting polymers. As the torsion angle between adjacent rings increases, the ionisation potential and band gap increase and the bandwidth of the highest occupied bands decreases. The evolution of these electronic properties, in particular the ionisation potential, can be well fitted by a cosine function. This indicates that in these conjugated systems, as expected, the electronic interactions between rings decrease as a function of the reduction of overlap between the p atomic orbitals on adjacent rings. The coplanar conformation is obviously the ideal for overlap and therefore maximum conductivity.

The solid state calculations were based on the structural properties measured in the gas phase and have shown that: (i) the molecules crystallise in the planar conformation which favours overlap and hence conduction, (ii) the relative angles between different molecules in the unit cell are in agreement with experimental results for oligomers containing up to $n = 8$ phenyl rings. The comparative study of the gas-phase and the solid-state calculations indicate that, although in the gas-phase the oligo(*p*-phenylene) structures are not coplanar, crystal packing favours coplanar conformations, which are consistent with maximum conductivity. Reasonable changes to the basis-sets and force-fields of the Molecular Orbital calculations or slight modifications to the constraints of the crystal packing calculations do not alter this general conclusion. Furthermore, predictions are given for the crystal structure of larger oligomers ($n = 10, 11$), that have yet to be crystallised.

Acknowledgements

The authors acknowledge financial support from the British-Greek bilateral scientific collaboration program ATH/882/2/POL on Conducting Polymers.

References

[1] Elsenbaumer RL, Shacklette LW. Handbook of conducting polymers. New York: Skotheim, 1986. p. 213–64.
[2] Shacklette LW, Chance RR, Ivory DM, Miller GG, Baughman RH. Synth Met 1979;1:307.
[3] Shacklette LW, Eckhardt H, Chance RR, Miller GG, Ivory DM, Baughman RH. J Chem Phys 1980;73:4098.
[4] Ivory DM, Miller GG, Sowa JM, Shacklette LW, Chance RR, Baughman RH. J Chem Phys 1979;7:1506.
[5] Delugeard Y, Desuche J, Baudour JL. Acta Crystallogr Sect B 1976; 32:702.
[6] Baudour JL, Cailleau H, Yelon WB. Acta Crystallogr Sect B 1977; 33:1773.
[7] Baudour JL, Delugeard Y, Rivet P. Acta Crystallogr Sect B 1978; 34:625.
[8] Pan J-F, Chua S-J, Huang W. Thin Solid Films 2000;363:1.
[9] Majewski JA, Vogl P, Leising P. Phys Rev B 1995;51:9668.
[10] Miao MS, Van Doren VE, van Camp PE, Straub G. Comput Mater Sci 1998;10:362.
[11] Champagne B, Mosley DH, Fripait J, Andre JM. Phys Rev B 1996;54:2381.
[12] Brédas J, Street GB, Themans B, Andre JM. J Chem Phys 1985; 83:1323.
[13] Majewski JA, Vogl P, Leising G. Phys Rev B 1995;54:2381.
[14] Sasaki S, Yamamoto T, Kanbara T, Morita A, Yamamoto T. J Polym Sci 1992;30:293.
[15] Leach AR. Molecular modelling, principles and applications. UK: Longman, 1996.
[16] Frisch MJ, Trucks GW, Schiegel HW, Gill PMW, Johnson BG, Wong MW, Foresman JB, Robb MA, Head-Gordon M, Replogle ES, Gompetts R, Andres JL, Raghavachari K, Binkley LS, Gonzalez G, Martin RL, Fox DL, Defrees DJ, Baker J, Stewart JJP, Pople J. J.A. Gaussian Inc., GAUSSIAN 94/DFT, Revision, Pittsburgh, PA, 1994.
[17] Cuff L, Kertesz M. Macromolecules 1994;27:762–70.
[18] Bredas JL, Salaneck WR, Stafstrom S. Conjugated polymer surfaces and interfaces and chemical structure of interfaces for polymer light emitting devices. Cambridge: Cambridge University Press, 1996.
[19] Almlof J. Chem Phys 1974;6:135.
[20] Bastiansen G. Acta Chem Scand 1949;3:408.
[21] Stolevik R, Thingstad G. J Mol Struct 1984;106:333.
[22] Dewar MJS, Zoebisch EG, Healy EF, Stewart JJ. J Am Chem Soc 1985;107:3902.
[23] Baker KN, Fratini AV, Resch T, Knachel HC, Adams WW, Socci EP, Farmer BL. Polymer 1993;34(8):1571.
[24] Allen MP, Tildesley DJ. Computer simulations of liquids. UK: Oxford Science Publications, 1987.
[25] Press WH, Flannery BP, Teukolsky SA, Vetterling WT. Numerical recipes in Fortran 77. UK: Cambridge University Press, 1992.